Synthesis and Characterization of Degradable Triarm Low Unsaturated Poly(propylene oxide)-*block*-polylactide Copolymers

Dongmei Yang,[1] Qi Lu,[1] Zhongyong Fan,[1] Suming Li,[1] Jianjun Tu,[2] Wei Wang[2]

[1]*Department of Materials Science, Fudan University, Shanghai 200433, People's Republic of China*
[2]*Department of Polymer Materials, Shanghai Research Institute of Petrochemical Technology, Shanghai 201208, People's Republic of China*

Received 20 June 2009; accepted 21 August 2009
DOI 10.1002/app.31336
Published online 22 June 2010 in Wiley InterScience (www.interscience.wiley.com).

ABSTRACT: A series of novel degradable triarm poly(propylene oxide)-*block*-polylactide (PPO-*b*-PLA) copolymers was synthesized by ring-opening polymerization of L-lactide (LLA) or D,L-lactide (DLLA) using low unsaturated PPO triols as macromolecular initiator. The chemical structures of the resulting copolymers were characterized by Fourier transform infrared (FTIR), gel permeation chromatography (GPC), and proton nuclear magnetic resonance (^{1}H-NMR) spectroscopy. Combination of FTIR, GPC, and NMR results confirmed the formation of PPO-*b*-PLA copolymers. One glass transition was observed by differential scanning calorimetry (DSC), suggesting good miscibility between PPO and PLA segments in the copolymers. DSC and wide-angle X-ray diffraction demonstrated that PPO-*b*-PLLA copolymers were semicrystalline materials, and the crystallinity increased with increasing the PLLA content. In contrast, PPO-*b*-PDLLA copolymers were totally amorphous. The PPO-*b*-PLA copolymers exhibited improved thermal stability when compared with PPO polyols according to thermogravimetric analysis. The thermal degradation behavior of the copolymers depended on the composition. Polyurethane foams were prepared by crosslinking PPO and PPO-*b*-PLA copolymers using isocyanate. Alkaline degradation of the foams was investigated in 10 wt/vol % NaOH at 80°C. The results show that the novel PPO-*b*-PLA copolymers could be promising as degradable polymeric materials. © 2010 Wiley Periodicals, Inc. J Appl Polym Sci 118: 2304–2313, 2010

Key words: structure; thermal properties; degradation

INTRODUCTION

During the last two decades, the development of degradable copolymers based on polylactide (PLA) has attracted much attention for both biomedical and environmental applications. These materials can be used in the fields of sustained drug delivery, gene delivery, osteosynthesis, and tissue engineering. They can also be used as engineering plastics with the aim of reducing environmental pollution related to plastic wastes. However, PLA is a hydrophobic and brittle polymer, which considerably restricts its potential applications. Hydrophilic and flexible polyether blocks have been incorporated into degradable polyesters. By combining the properties of both components, materials with suitable hydrophilicity, degradability, mechanical and biological properties can be achieved. Poly(ethylene glycol) or poly(ethylene oxide) (PEO) has been used as a source of hydrophilicity due to the outstanding physicochemical and biological properties including solubility in water and in organic solvents, nontoxicity, and filterability through kidney when the molar mass is below 30,000. The glass transition temperature (T_g) of PLA plasticized with PEO can be efficiently reduced by about 30–70°C, and various PLA/PEO block copolymers have been prepared and investigated as drug carriers in the form of microparticles, nanoparticles, micelles, and hydrogels.[1–3] However, phase separation due to crystallization of PEO segment in PLA/PEO copolymers was found to affect the material properties, such as increased stiffness and decreased elongation at break.

Poly(propylene oxide) (PPO) is an amorphous polymer with a very low glass transition temperature (about −75°C).[4] PPO is miscible with PLA, which makes it an attractive plasticizer for PLA processing. Piorkowska and Galeski[5,6] investigated the role of PPO segment in the plasticization of PLA in PPO/PLA blends. PLA was blended with PPO with molecular weight of 425 and 1000 g/mol. The PLA/PPO blends exhibit lower glass transition temperature, lower yield stress, and higher elongation at break when compared with pure PLA. PPO/PLA

Correspondence to: Z. Fan (zyfan@fudan.edu.cn).
Contract grant sponsor: Chinese National Nature Science Foundation; contract grant numbers: 20474013, 20674013.
Contract grant sponsor: Shanghai Leading Academic Discipline Project; contract grant number: B113.

© 2010 Wiley Periodicals, Inc.

copolymers have been synthesized by ring-opening polymerization of lactides and propylene oxide using different catalysts.[7] The ring-opening mechanism of PO and lactides was discussed. PPO/PLA block copolymers were obtained by consecutive reactions of both cyclic monomers. Aubrecht and Grubbs prepared (PEO-*stat*-PPO)-*b*-PLA diblock and PEO-*b*-(PEO-*stat*-PPO)-*b*-PLA triblock copolymers by ring-opening polymerization of LA using BuO-(PEO-*stat*-PPO)-OH and MeO-PEO-*b*-(PEO-*stat*-PPO)-OH as macroinitiators and $AlEt_3$ as catalyst.[8] The block copolymers were incorporated with PEO-*stat*-PPO blocks to prepare thermoresponsive amphiphilic materials used as stimuli-responsive polymeric micelles in aqueous solution.

Low unsaturated PPO triols are well known commercial chemicals, whose most important application is polyurethane production.[9–12] In the past, PPO polyols have been prepared using simple and inexpensive catalysts such as sodium and potassium hydroxides or alkoxides. During oxypropylation, propylene oxide is subjected to a competing internal rearrangement, which generates unsaturated alcohols. The resulting products usually contain unsaturated, monohydroxyl-functional species, leading to lower functionality and wide molecular weight (M_w) distribution. Many attempts have been made to lower the degree of unsaturation.[13–15] Recently, low unsaturated PPO polyols with narrow M_w distribution have been prepared by double metal cyanide complex oxyalkylation catalysts.[16–18] It has been proved that flexible slabstock polyurethane foams synthesized from low unsaturated polyoxyalkylene polyethers have substantially improved indentation force deflection and resilience characteristics while maintaining other physical properties unchanged.[19,20]

The purpose of this work was to synthesize PPO-*b*-PLA copolymers by ring-opening polymerization of LLA or DLLA using low unsaturated PPO as macroinitiator. The chemical structure and the composition of the copolymers were characterized by FTIR, GPC, and ^{1}H-NMR. The thermal properties were investigated by differential scanning calorimetry (DSC) and thermogravimetric analysis (TGA), and the crystallization behaviors and crystal structure were determined by DSC and wide-angle X-ray diffraction (WAXD). In addition, the alkaline degradability of flexible polyurethane foams containing PPO-*b*-PLA block copolymers is also reported.

EXPERIMENTAL

Materials

Low unsaturated PPO triol with number average molecular weight ($\overline{M}_n$) of 3300 was supplied by Shanghai Research Institute of Petrochemical Technology.[21] The maximal degree of unsaturation of PPO is less than 0.01 mmol/g. PPO was dehydrated and degassed under vacuum at 105°C for 90 min and was stored under dried nitrogen before use. Lactic acid (LA), zinc powder, and stannous octoate ($Sn(Oct)_2$) were purchased from Sinopharm Chemical Reagent. Toluene diisocyanate mixture (80% of 2,4-isomer and 20% of 2,6-isomer, TDI-80), 33% diaminobicyclooctane in dipropylene glycol (A-33), and surfactant (B8110) were supplied by Evonic (China) and used as received.

Synthesis of L- and D,L-lactide

Both L- and D,L-lactide were synthesized by using a two-step procedure: LA was first condensed to yield low-molecular weight prepolymers, lactide was then formed by depolymerization of the prepolymers. Briefly, 250 mL of L- or D,L-LA and 0.3 wt % zinc powder were charged into a 500 mL dried flask. The mixture was slowly heated from 90 to 110°C under about 400 mmHg to remove residual water during 2 h. Then the temperature was gradually increased up to 180°C at a heating rate of 10°C every 30 min, and the condensation reaction was allowed to proceed for about 3.5 h. After that, depolymerization was carried out under a lower pressure of about 40 mmHg. The temperature was slowly increased from 180 to 220°C. The reaction was stopped when no distillation was detected. Finally, crude lactide was recrystallized from ethyl acetate for four times, followed by vacuum drying up to constant weight.

Synthesis of PPO-*b*-PLA block copolymer and PLA homopolymer

PPO-*b*-PLLA or PPO-*b*-PDLLA copolymers were synthesized by ring-opening polymerization of lactide using $Sn(Oct)_2$ as catalyst and PPO triol as macroinitiator. Lactide, PPO, and 0.1 wt % of catalyst were transferred into a round-bottomed flask. After purged with nitrogen three times, the flask was sealed under vacuum (below 10^{-3} mmHg). The polymerization was then allowed to proceed at 140°C for 7 days. The copolymers thus obtained were dissolved in dichloromethane and precipitated with methanol, followed by vacuum drying up to constant weight. Four PPO-*b*-PLA copolymers were synthesized with the PO/LA molar ratios (n_{PO}/n_{LA}) of 2/1 and 1/1, and were abbreviated as PPO-*b*-PLLA 2/1, PPO-*b*-PLLA 1/1, PPO-*b*-PDLLA 2/1, and PPO-*b*-PDLLA 1/1, respectively.

As reference samples, PLLA and PDLLA homopolymers were synthesized by ring-opening polymerization of L-lactide or D,L-lactide, using $Sn(Oct)_2$ as catalyst and octanol as initiator. The L-lactide or

D,L-lactide/octanol molar ratio was 69/1. Polymerization was performed at 140°C for 2 days. The obtained homopolymers were purified by the dissolution/precipitation method mentioned earlier. The $\overline{M}_n$ value determined by GPC was 18,200 for PLLA, and 17,200 for PDLLA.

Preparation of polyurethane foams containing PPO-*b*-PLA block copolymers

PPO, isocyanate, and PPO-*b*-PLA copolymers were maintained at 20–25°C before use. PPO triols were mixed with 36.0 wt % of PPO-*b*-PLLA 2/1 or PPO-*b*-PDLLA 2/1 copolymers, or with 25 wt % of PPO-*b*-PLLA 1/1 or PPO-*b*-PDLLA 1/1 copolymers, for the PPO content of the polyol mixture was a constant about 86.2 wt %. The polyol mixture, water (blowing agent, 4.2 wt %), A-33 (catalyst, 0.2 wt %), $Sn(Oct)_2$ (catalyst, 0.2 wt %), and B8110 (surfactant, 1.2 wt %) were charged into a stainless steel container and stirred for 60 s at 1300 rpm. The formulation was based on the total PPO content. Then, a predetermined amount of isocyanate was rapidly poured into the container and the reactants were mixed thoroughly for 7 s with a high-speed stirrer at 2000 rpm. The amount of isocyanate is determined by the following equation:

$$n_{-\mathrm{NCO}} = 1.05 \times (n_{-\mathrm{OH}}(\mathrm{polyol}) + 2 \times n_{\mathrm{water}}) \quad (1)$$

where $n_{-\mathrm{NCO}}$ is the number of moles of —NCO, $n_{-\mathrm{OH}}$(polyol) is the number of moles of —OH from PPO and PPO-*b*-PLA copolymer polyols, and n_{water} is the number of moles of water. The reactants were rapidly poured into a mold with dimensions of 250 × 250 × 250 mm^3. The mold was kept at room temperature for 10 min, and polyurethane foam was formed by blowing and gelling reactions. The foam was allowed to fully develop with an additional 1 h cure at 100°C. After curing, the polyurethane foams were kept at room temperature for 1 week before degradation experiments. For the sake of simplicity, the foams are named as PU-L21, PU-L11, PU-DL21, and PU-DL11, where L and DL stand for PPO-*b*-PLLA and PPO-*b*-PDLLA copolymers, and 21 and 11 indicate that the PO/LA monomer molar ratio is 2/1 and 1/1, respectively. A polyurethane foam without PLA segment (named PU0) was also synthesized from PPO only for comparison.

Hydrolytic degradation of polyurethane foams

PU-LA foam samples with dimensions of 20 × 20 × 10 mm^3 were placed into a small flask filled with 25 mL of 10 wt/vol % NaOH at 80°C. At each degradation time, three specimens were withdrawn, washed with deionized water, and then dried under vacuum at 45°C for a week before weighing. The degradability is estimated from the weight loss of the samples:

$$\mathrm{Weightloss}\% = (W_0 - W_t)/W_0 \times 100\% \quad (2)$$

where W_0 is the weight of the original samples and W_t is the weight of residual samples after the degradation for various time.

Characterization

The specific optical rotation of lactide monomers, [α], was measured at 20°C in dichloromethane at a concentration of 8.6–9.0 mg/mL with a WZZ-2S digital automatic spectropolarimeter at a wavelength of 578 nm. The [α] values of L-lactide and D,L-lactide were found to be −261 and 0, corresponding to a L-lactide content of 96.1 and 50.0 wt %, respectively.

Fourier transform infrared (FTIR) spectroscopy was carried out with a Nicolet Magna-IR560 FTIR spectrometer with a resolution of 2 cm^{-1} in the range from 400 to 4000 cm^{-1}.

The molecular weights were measured at 40°C with gel permeation chromatography (GPC) on PerkinElmer Series 200GPC System using polystyrene standards. Chloroform was used as the eluent at a flow rate of 1.0 mL/min.

Proton nuclear magnetic resonance (^{1}H-NMR) spectra were recorded on a BRUKER spectrometer at 400 MHz. Deuterated chloroform was used as the solvent, and tetramethylsilane as the internal standard.

DSC was performed with a Dupont instrument DSC 910 under N_2 atmosphere. The samples were first heated up to 250°C and kept for 2 min, followed by quenching in liquid nitrogen. A second run was then performed from −80 to 250°C at a heating rate of 10°C/min.

WAXD measurements were carried out with a Bruker D8 advance diffractometer equipped with a scintillation counter, using CuKα radiation with a wavelength of 0.1542 nm. The instrument was operated at an excitation voltage of 40 kV and a current of 40 mA. The scanning rate was 4 deg/min, and the spectra were recorded at a resolution of 0.02°.

TGA measurements were carried out with a Dupont instrument TGA 951 at a heating rate of 10°C/min under air atmosphere.

Microstructure of the samples was examined with a SUPERSCAN SSX-550 scanning electron microscope (SEM). Thin foam slices, about 5 mm, were mounted to aluminum stubs using copper tape. Before SEM observation, a thin layer of Au, about 5 nm, was electrically deposited to enhance the conductivity of the sample.

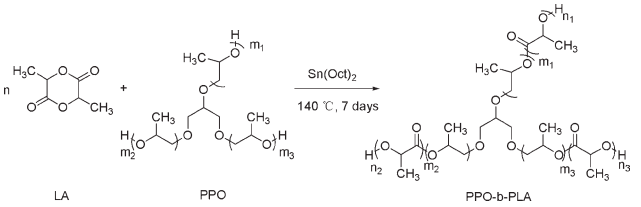

Scheme 1 Synthesis of PPO-*b*-PLA copolymers.

RESULTS AND DISCUSSION

Chemical structure and composition of PPO-*b*-PLA copolymers

The copolymers were prepared by ring-opening polymerization of L-lactide or D,L-lactide using low unsaturated PPO triols as macroinitiator at various molar ratios, as shown in Scheme 1. The resulting copolymers were characterized by FTIR, ^{1}H-NMR, and GPC. Figure 1 presents the FTIR spectra of PPO-*b*-PLLA 2/1, PPO-*b*-PLLA 1/1, and PPO. The broad absorbance bands in the range of 3600–3400 cm^{-1} indicate the presence of the OH groups. The absorbance bands in the range of 3000–2800 cm^{-1} are assigned to the C—H stretching. PLLA segments in the copolymers present strong absorbance bands in the range of 1750–1735 cm^{-1} due to carbonyl groups,[22] and two strong absorbance bands of the C—O stretching in the range of 1300–1050 cm^{-1} [Fig. 1(a,b)], confirming the formation of polyester blocks. PPO exhibits only a strong absorbance at 1100 cm^{-1} in the range of 1300–1050 cm^{-1} (Fig. 1c), which is characteristic of the C—O—C (ether) groups of PPO. Compared with the FTIR spectrum of pure PPO, the absorbance bands in the range of 1300–1170 cm^{-1} are ascribed to the C—O bond of the PLA segments, and 1170–1050 cm^{-1} to the C—O bond of both PLA and PPO segments. On the basis of the intensity of the absorbance bands in the range of 1170–1050 cm^{-1}, the relative absorbance intensity in the range of 1300–1170 cm^{-1} of PPO-*b*-PLLA 1/1 is much higher than that of PPO-*b*-PLLA 2/1, in agreement with higher PLLA content. Similar results are obtained for the PPO-*b*-PDLLA copolymers. Therefore, the FTIR spectra evidence the formation of PPO-*b*-PLA block copolymers.

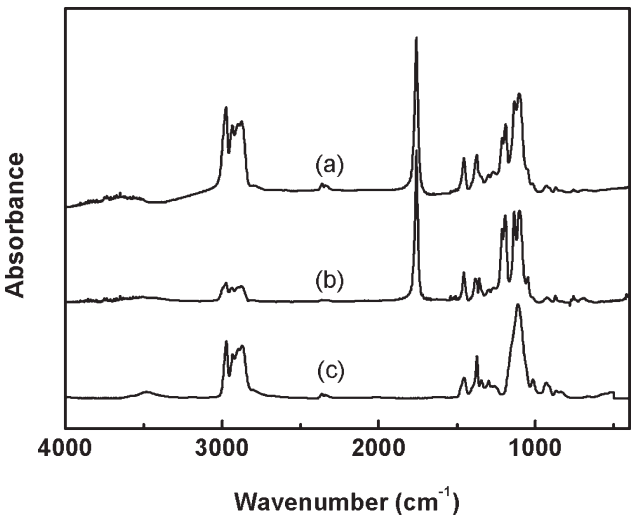

Figure 1 FTIR spectra of PPO-*b*-PLLA copolymers and PPO (a) PPO-*b*-PLLA 2/1, (b) PPO-*b*-PLLA 1/1, and (c) PPO.

GPC is an important method for the determination of molecular weight and molecular-weight distribution of polymers. The molecular weights of the copolymers measured by GPC are listed in Table I. The $\overline{M}_n$ of the macroinitiator PPO is 3300 as determined by GPC. The $\overline{M}_n$ values of the PPO-*b*-PLLA and PPO-*b*-PDLLA copolymers are in the range of 5400–10,100. Furthermore, both the $\overline{M}_n$ and the weight average molecular weight ($\overline{M}_w$) increase with the PLA content in the copolymers. The copolymers all presented monodisperse curves with polydispersity index (PDI) in the range of 1.03–1.09. Similar results were obtained in the previous articles where $Sn(Oct)_2$ was used as catalyst for the ring-opening polymerization of L-lactide initiated by alcohol, such as pentaerythritol[23] or glycerol.[24]

^{1}H-NMR was used to determine the chain structure, composition, and absolute molecular weight of the copolymers. ^{1}H-NMR spectra of PPO-*b*-PLLA 2/1 and PPO are shown in Figure 2. Comparative analysis of the spectra allows complete assignment of all the signals. From the ^{1}H-NMR spectrum of PPO [Fig. 2(b)], the signals at 1.09 ppm are assigned to the methyl protons of PPO, and those 3.36–3.51 ppm to the methine and methylene protons of both PPO

TABLE I
Molecular Characteristics of PPO-*b*-PLA Copolymers Determined by GPC and ^{1}H-NMR

Samples	GPC			^{1}H-NMR		
	$\overline{M}_n(\times10^3)$	$\overline{M}_w(\times10^3)$	PDI	n_{PO}/n_{LA}	DP_{PLA}	$\overline{M}_n(\times10^3)$
PPO-*b*-PLLA 2/1	5.9	6.0	1.03	1.73	24.1	4.2
PPO-*b*-PLLA 1/1	10.1	11.1	1.09	0.74	56.6	6.6
PPO-*b*-PDLLA 2/1	5.4	5.7	1.07	1.76	23.8	4.2
PPO-*b*-PDLLA 1/1	6.2	6.8	1.09	0.96	43.2	5.6

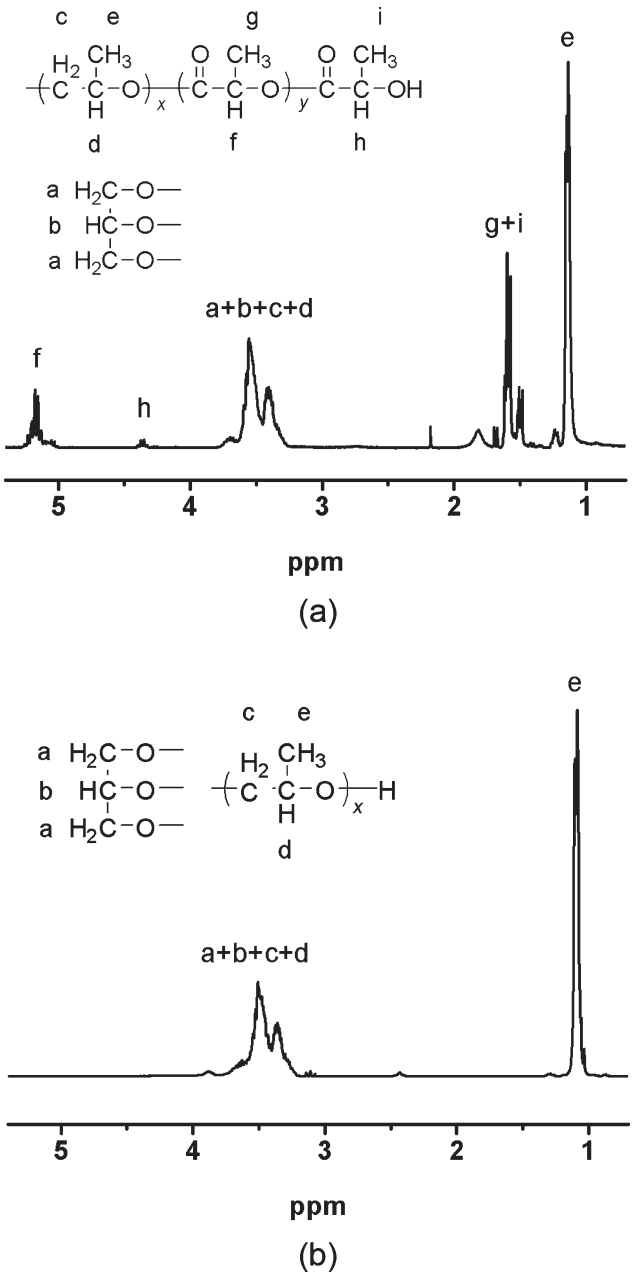

Figure 2 ^{1}H-NMR spectra of PPO-*b*-PLA copolymer and PPO: (a) PPO-*b*-PLLA 2/1 and (b) PPO.

and glycerol (GL, the initiator of PPO triol), respectively.[25] The PO/GL molar ratio (n_{PO}/n_{GL}) or the mean number average degree of polymerization of the PPO segments (DP_{PPO}), and the $\overline{M}_n$ of PPO ($\overline{M}_{nPPO}$) can be obtained from the following equations:

$$n_{PO}/n_{GL} = DP_{PPO} = (I_e/3)/((I_{a+b+c+d} - I_e)/5) \quad (3)$$

$$\overline{M}_{nPPO} = 58 \times DP_{PPO} + 92 \quad (4)$$

where I represents the integration intensities, the subscript stands for different protons, and 58 and 92 are the molecular weights of PO repeat units and glycerol, respectively. The value of DP_{PPO} is found to be 41.7, and the $\overline{M}_{nPPO}$ is 2511, that is slightly lower than the GPC result which is based on polystyrene standards.

In the ^{1}H-NMR spectrum of PPO-*b*-PLLA 2/1 [Fig. 2(a)], the resonance signals at 1.14 ppm are assigned to the methyl protons of PO units, and the signals around 1.60 ppm to the methyl protons of LLA units.[24,26] The signals of the methine and methylene protons of glycerol and PO units are detected in the range of 3.4–3.7 ppm. The signals at 4.35 ppm are assigned to the methine protons of LLA end units, and those at 5.18 ppm to the methine groups of LLA main chain units.[24,26]

The PO/LA molar ratio (n_{PO}/n_{LA}) in the PPO-*b*-PLA copolymers, the mean number average degree of polymerization of the PLA segments (DP_{PLA}), and the $\overline{M}_n$ of the copolymers are determined using the integration intensities of the methyl protons of PO units and the methine protons of LLA units, as shown in the following equations:

$$n_{PO}/n_{LA} = (I_e/3)/(I_f + I_h) \quad (5)$$

$$DP_{PLA} = DP_{PPO}/(n_{PO}/n_{LA}) \quad (6)$$

$$\overline{M}_n = \overline{M}_{nPPO} + 72 \times DP_{PLA} \quad (7)$$

where 72 is the molecular weight of LA repeat units. The results are summarized in Table I. According to eq. (6), the lower the n_{PO}/n_{LA}, the higher the DP_{PLA}, as DP_{PPO} is a constant (41.7). Similarly, eq. (7) suggests that the $\overline{M}_n$ of the copolymers increases with the DP_{PLA} value since the ^{1}H-NMR derived $\overline{M}_{nPPO}$ is a constant (2511). The $\overline{M}_n$ values determined by ^{1}H-NMR range from 4221 to 6585 for the PPO-*b*-PLA copolymers. Therefore, combination of FTIR, GPC,

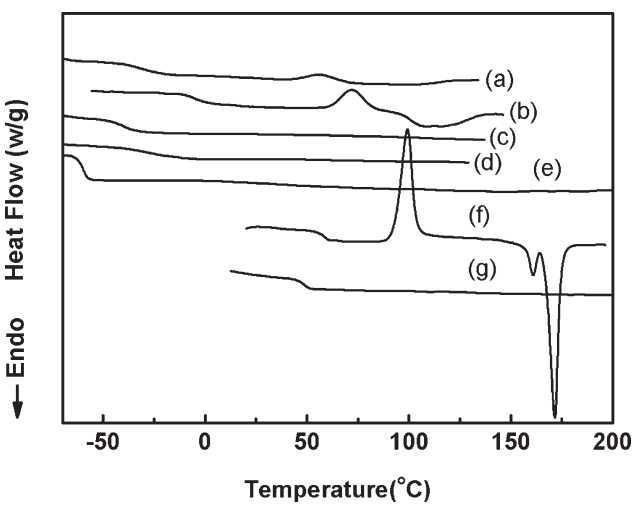

Figure 3 DSC curves of PPO-*b*-PLA copolymers, PPO, PLLA, and PDLLA: (a) PPO-*b*-PLLA 2/1, (b) PPO-*b*-PLLA 1/1, (c) PPO-*b*-PDLLA 2/1, (d) PPO-*b*-PDLLA 1/1, (e) PPO, (f) PLLA, and (g) PDLLA.

TABLE II
Thermal Properties, Crystallinity, and Lamellar Thickness of PPO-*b*-PLLA Copolymers and PLLA

Samples	T_g (°C)	T_c (°C)	ΔH_c (J/g)	T_m (°C)	ΔH_m (J/g)	X_c (%)	l (nm)
PPO-*b*-PLLA 2/1	−32.8	55.7	5.2	94.7	5.6	6.4	4.7
PPO-*b*-PLLA 1/1	−14.9	64.8	12.8	105.2	15.7	18.0	5.2
PLLA	58.8	99.4	42.8	171.7	57.7	66.3	14.9

and NMR data suggests that PPO-*b*-PLA copolymers were successfully obtained by ring-opening polymerization of lactide initiated by PPO triol.

Glass transition temperature of PPO-*b*-PLA copolymers

The glass transition temperature (T_g) of the PPO-*b*-PLA copolymers was evaluated by DSC, and a second run was performed to determine the thermal properties of the copolymers (Fig. 3). The T_g of PPO initiated by glycerol is detected at −59.6°C, in agreement with the flexibility of PPO chains [Fig. 3(e)]. While with relatively rigid backbones, PLLA and PDLLA homopolymers exhibit a glass transition at 58.8 and 48.8°C [Fig. 3(f,g)], respectively. In the case of the copolymers, T_g is detected at −32.8°C for PPO-*b*-PLLA 2/1, at −14.9°C for PPO-*b*-PLLA 1/1, at −38.8°C for PPO-*b*-PDLLA 2/1, and at −29.3°C for PPO-*b*-PDLLA 1/1. In general, the glass transition temperature of copolymers strongly depends on the composition and the chemical structure of the components. From the DSC curves, a single glass transition between those of corresponding homopolymers is observed for the PPO-*b*-PLLA and PPO-*b*-PDLLA copolymers, suggesting good miscibility between the PPO segments and the PLLA or PDLLA segments. The T_gs of the copolymers are higher than that of PPO homopolymer, and increase with increasing PLA content or DP_{PLA}, because of chain rigidification with attachment of PLA segments. On the other hand, flexible PPO segments exert plasticization effects on rigid PLA segments. Therefore, the T_g of the copolymers decreases by about 70–90°C, compared with PLA homopolymers.

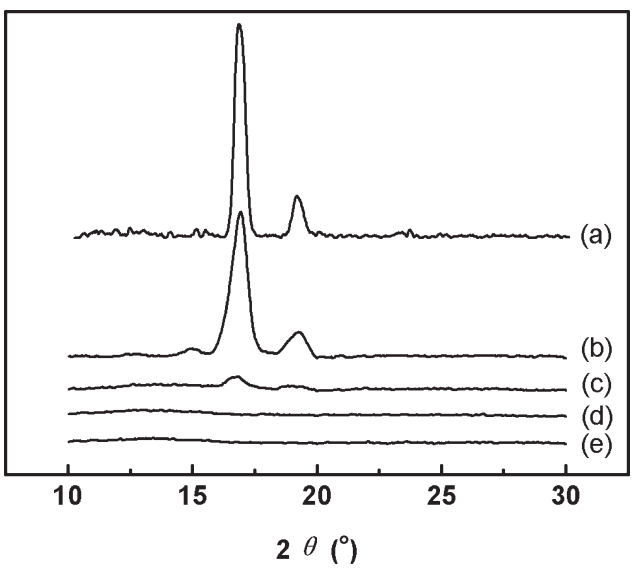

Figure 4 Wide-angle X-ray diffraction (WAXD) patterns of PPO-*b*-PLA copolymers: (a) PLLA, (b) PPO-*b*-PLLA 1/1, (c) PPO-*b*-PLLA 2/1, (d) PPO-*b*-PDLLA 1/1, and (e) PPO-*b*-PDLLA 2/1.

Crystallization behavior of the copolymers

The chemical structure of a polymer determines whether it will be able to crystallize. Generally, symmetrical chain structures favor crystallinity, whereas asymmetrical chain structures hinder crystallization. PPO with asymmetrically placed methyl groups is intrinsically amorphous, as proved by DSC [Fig. 3(e)]. In the case of PLA polymers, the crystallization behavior depends on the stereochemical structure. PDLLA is unable to crystallize because it is synthesized from an equimolar mixture of L- and D-lactides and thus exhibits low stereoregularity [Fig. 3(g)]. As a consequence, PPO-*b*-PDLLA copolymers are also intrinsically amorphous materials [Fig. 3(c,d)].

PLLA homopolymer was obtained from a mixture containing 96.1% L-lactide. It is able to crystallize because of its high stereoregularity. A crystallization

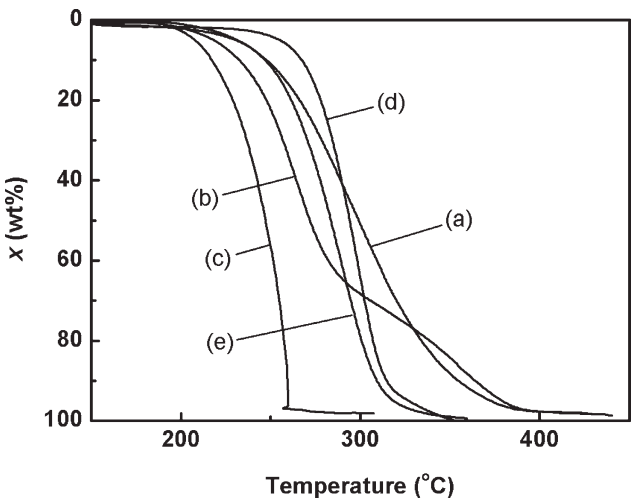

Figure 5 TGA curves of PPO-*b*-PLA copolymers, PPO, PLLA, and PDLLA: (a) PPO-*b*-PLLA 2/1, (b) PPO-*b*-PDLLA 2/1, (c) PPO, (d) PLLA, and (e) PDLLA.

TABLE III
Thermal Decomposition Data of PPO-*b*-PLA Copolymers, PPO, PLLA, and PDLLA Determined by TGA

Samples	T_{di} (°C)	$(dx/dT)_{m1}$ (%/°C)	T_{dm1} (°C)	$(dx/dT)_{m2}$ (%/°C)	T_{dm2} (°C)
PPO-*b*-PLLA 2/1	249	0.99	296	–	–
PPO-*b*-PLLA 1/1	255	1.43	297	–	–
PPO-*b*-PDLLA 2/1	235	1.32	266	0.41	362
PPO-*b*-PDLLA 1/1	241	0.92	270	0.71	382
PPO	207	11.70	257	–	–
PLLA	271	2.48	299	–	–
PDLLA	243	1.84	289	–	–

T_{di} is the intersection temperature of the baseline and the tangent of decomposition curve.

temperature (T_c) is observed at 99.4°C and a melting temperature (T_m) at 171.7°C [Fig. 3(f)]. PPO-*b*-PLLA copolymers are also semicrystalline. However, the T_c decreases to 55.7°C for PPO-*b*-PLLA 2/1 and to 64.8°C for PPO-*b*-PLLA 1/1. In principle, a semicrystalline polymer is able to crystallize above its T_g. The difference between T_c and T_g reflects the crystallization ability. This difference is 40.6 for PLLA, 79.7 for PPO-*b*-PLLA 1/1, and 88.5 for PPO-*b*-PLLA 2/1. Therefore, attachment of PPO segments disfavors crystallization of PLLA. Similarly, T_m and ΔH_m of the PPO-*b*-PLLA copolymers are much lower than those of PLLA homopolymer. PPO-*b*-PLLA 2/1 presents lower T_m and ΔH_m than PPO-*b*-PLLA 1/1 because of lower DP_{PLA} of the former. All the thermal property data are listed in Table II.

The equilibrium melting temperature (T_m^0) of a polymer is the temperature at which the chemical potential of the polymeric units in the crystalline phase is equal to that in the melt.[27] In fact, the value of T_m^0 is usually defined as the melting temperature of lamellae of infinite thickness. The lamellar thickness (l) can be estimated from $l = \frac{2\sigma_e T_m^0}{\Delta H(T_m^0 - T_m)}$.[28] Here σ_e is the fold surface free energy (for PLLA, $\sigma_e = 6.09 \times 10^{-2}$ J/m^2),[29] ΔH is the heat of fusion per unit volume (for PLLA, $\Delta H = 1.11 \times 10^8$ J/m^3),[29] and T_m^0 for PLLA is 207°C.[29,30] The lamellar thickness of PLLA is estimated to be 14.9 nm (Table II). In contrast, much lower lamellar thickness values were obtained for the copolymers, that is, 5.2 nm for PPO-*b*-PLLA 1/1 and 4.7 nm for PPO-*b*-PLLA 2/1. These findings indicate that the perfection of PLLA crystals in PPO-*b*-PLLA copolymers decreases due to attachment of PPO segments. PPO-*b*-PLLA 1/1 presents higher lamellar thickness than PPO-*b*-PLLA 2/1 because of higher DP_{PLA} of the former.

The degree of crystallinity (X_c%) for the PLLA segments in the PPO-*b*-PLLA copolymers is calculated by using $X_c\% = \frac{\Delta H_m}{\Delta H_m^0} \times 100\%$, where ΔH_m is the enthalpy of melting (J/g), and ΔH_m^0 is the enthalpy of melting for a completely crystallized PLLA homopolymer (J/g). The value of 87 J/g is used as ΔH_m^0 of PLLA.[31] The degree of crystallinity is estimated to be 66.3% for PLLA homopolymer. The copolymers present much lower crystallinity, that is, 18.8% and 6.4% for PPO-*b*-PLLA 1/1 and PPO-*b*-PLLA 2/1, respectively, due to the presence of flexible PPO segments.

WAXD measurements were carried out to examine the crystal structure and dimensions of the PPO-*b*-PLLA copolymers. The diffraction patterns of the copolymers are presented in Figure 4. The PPO-*b*-PLLA copolymers are more or less crystalline with the presence of well-defined diffraction peaks. The (110)/(200) and (203) reflections appear at $2\theta = 16.8°$ and 19.2°, respectively, corresponding to α crystal cell of PLLA.[32–40] The reflections of PPO-*b*-PLLA 1/1 is much stronger and sharper than those of PPO-*b*-PLLA 2/1, indicating higher perfection of lamellae with higher crystallinity of PPO-*b*-PLLA 1/1, in agreement with DSC derived results. In comparison with the PPO-*b*-PLLA copolymers, the PPO-*b*-PDLLA copolymers appear totally amorphous with a broad amorphous halo.

On the basis of the half-height width of the (110)/(200) reflections, the average lateral size of crystal particles (L) of the PPO-*b*-PLLA copolymers can be calculated by using Scherrer equation,[41] $L = K\lambda/(\beta \cos \theta)$. Here λ is the wave length of the incident X-rays, β is the half-height width of the

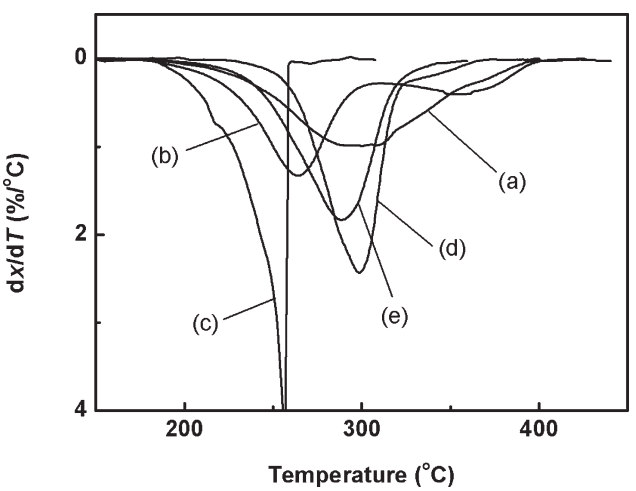

Figure 6 DTG curves of PPO-*b*-PLA copolymers, PPO, PLLA, and PDLLA: (a) PPO-*b*-PLLA 2/1, (b) PPO-*b*-PDLLA 2/1, (c) PPO, (d) PLLA, and (e) PDLLA.

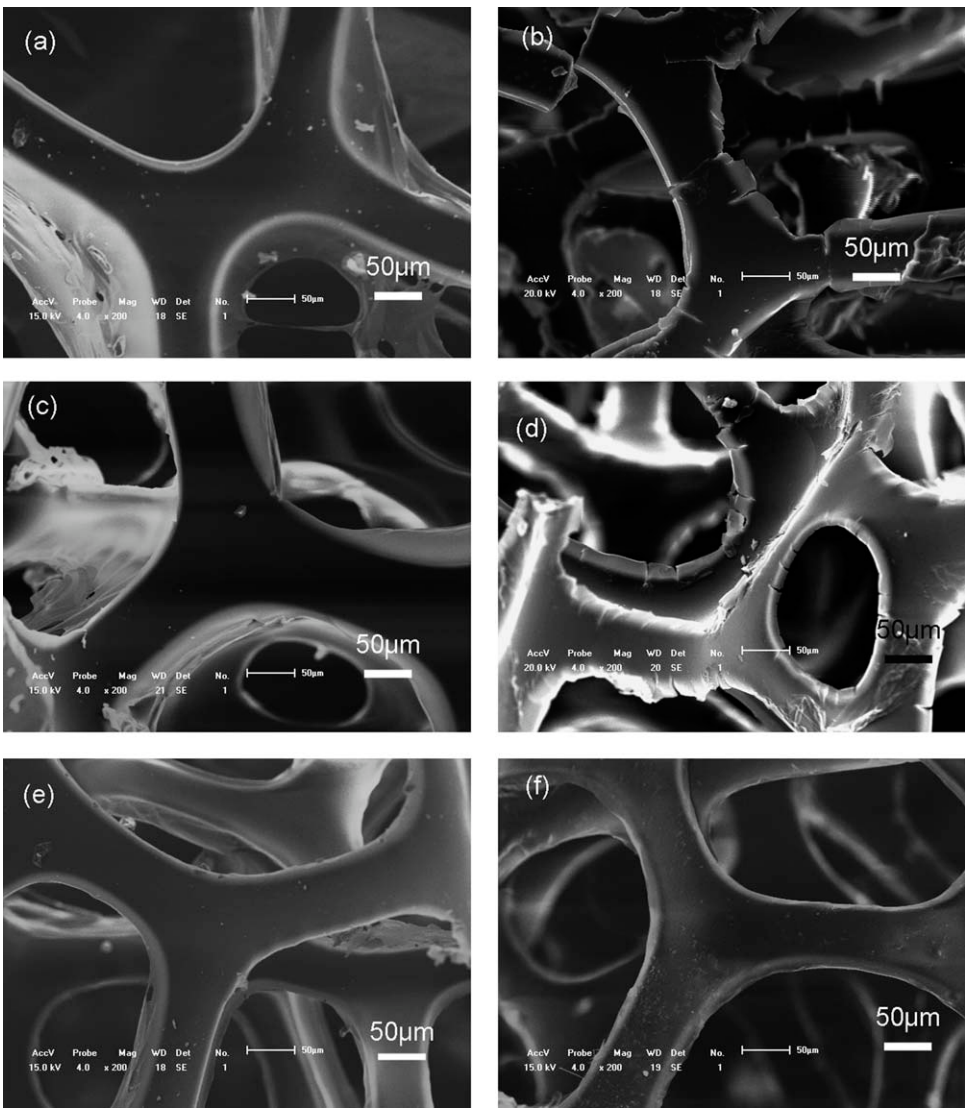

Figure 7 SEM photographs of PU foams of original samples and after alkaline hydrolysis in 10 wt/vol % NaOH solution at 80°C for 15 h: (a) original PU-L11, (b) PU-L11 after degradation, (c) original PU-DL11, (d) PU-DL11 after degradation, (e) original PU0, and (f) PU0 after degradation.

diffraction peaks, θ is the diffraction angle, and $K = 0.9$ is a constant.[41] The L value for PLLA homopolymer is 12.6 nm. Because of the attachment of flexible PPO segments, the regularity of the PLLA crystal particles decreases. As a result, the L values for PPO-*b*-PLLA 2/1 and PPO-*b*-PLLA 1/1 are 8.6 and 10.5 nm, respectively. Furthermore, the crystal size increases with increasing the PLLA content in the PPO-*b*-PLLA copolymers.

Thermal stability of PPO-*b*-PLA copolymers

TGA has been widely used to investigate the thermal stability and the decomposition characteristics of materials. Figure 5 presents the TGA curves of the PPO-*b*-PLA copolymers and PPO, PLLA, and PDLLA homopolymers. The thermal decomposition data are summarized in Table III. With rigid chemical structures, the thermal stability of PLLA or PDLLA homopolymer is higher than that of flexible PPO homopolymer. The initial decomposition temperature (T_{di}) of PPO is 207°C, and those of PLLA and PDLLA homopolymers are 271°C and 243°C, respectively. PLLA with higher stereoregularity is thermally more stable than PDLLA. In the case of the copolymers, the thermal stability is intermediate of the corresponding parent homopolymers. The PPO-*b*-PLLA copolymers present higher thermal stability than the PPO-*b*-PDLLA ones with the same monomer molar ratio, and the T_{di} value is higher for copolymers with higher PLA contents. It can be concluded that both the PLLA and PDLLA segments contribute to improve the thermal stability of the copolymers, and the contribution of highly

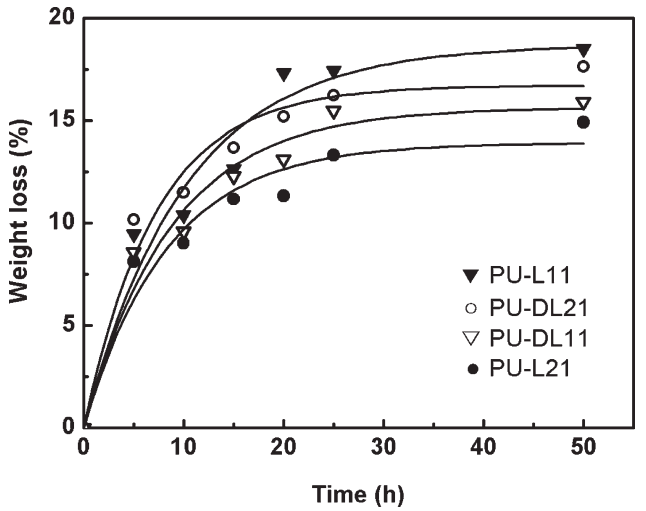

Figure 8 Weight loss changes of PU-LA foams in 10 wt/vol % NaOH solution at 80°C.

stereoregular PLLA segments is larger than that of less stereoregular PDLLA ones.

The derivative thermogravimetry (DTG) curves are shown in Figure 6. dx/dT stands for the decomposition rate of the polymers, $(dx/dT)_m$ the maximum decomposition rate, and T_{dm} the temperature at the maximum decomposition rate. The detailed data are listed in Table III. PPO exhibits an accelerated process throughout the whole decomposition range, and has a relatively high $(dx/dT)_m$ value (about 11.70%/°C) and low T_{dm} value (about 257°C), suggesting that PPO tends to undergo thermal decomposition. PLLA and PDLLA homopolymer show a single DTG peak, in agreement with a random thermal decomposition along the polymer backbone. The T_{dm} of PLLA (about 299°C) is 10°C higher than that of PDLLA, which is consistent with the T_{di} results. Two peaks are observed on the DTG curves of PPO-*b*-PLLA 2/1 and PPO-*b*-PDLLA 2/1 copolymers [Fig. 6(a,b)], indicating that the thermal decomposition consists of two chemical reactions, in the range of 200–315°C as reaction I and 315–425°C as reaction II. Reaction I, occurring at lower temperature, is caused by the ether bonds destruction in the PPO segments. And reaction II, at higher temperature, is assigned to the ester bonds destruction in the PLA segments. With increasing PLLA or PDLLA content in the copolymers, the weight loss contribution in the range of 200–315°C becomes lower, and that in the range of 315–425°C becomes more important. It is noted that with higher stereoregularity of the PLLA segments, the T_{dm} values of reaction II of the PPO-*b*-PLLA copolymers are about 30°C higher than those of the PPO-*b*-PDLLA ones with the same monomer molar ratio. Reaction II of the PPO-*b*-PLLA copolymers almost overlaps with reaction I. Thus, the T_{dm} values of reaction II of the PPO-*b*-PLLA copolymers are hardly distinguishable. In the case of PPO-*b*-PDLLA copolymers, thermal decomposition of the PPO segments first occurs at lower temperature, followed by that of the PDLLA segments at higher temperature.

Degradation of polyurethane foams containing PPO-*b*-PLA block copolymers

To evaluate the degradability of polyurethane foams containing PPO-*b*-PLA block copolymers, alkaline hydrolysis experiments were performed in 10 wt/vol % NaOH solution at 80°C. SEM was used to monitor the changes of the strut structures of the PU foams of original samples and after alkaline hydrolysis for 15 h. First of all, it was observed that the strut structures of original PU-L11, PU-DL11, and PU0 were well-formed and integrated [Fig. 7(a,c,e)]. While after degradation in 10 wt/vol % NaOH solution at 80°C for 15 h, the strut structures of PU0 almost unchanged [Fig. 7(f)], indicating that no degradation behavior occurred for PU0. On the contrary, decayed struts structures of PU-L11 and PU-DL11 were observed under the same degradation conditions [Fig. 7(b,d)], suggesting that degradation took place for PU foams containing PPO-*b*-PLLA 1/1 or PPO-*b*-PDLLA 1/1. To quantitatively measure the degradability, the weight-loss of the samples was recorded after alkaline hydrolysis for different time. Figure 8 shows the corresponding weight-loss data. It appears that the weight-loss percentages of the polyurethane foams containing PPO-*b*-PLLA or PPO-*b*-PDLLA copolymers increased rapidly during the first 15 h, and then attained a constant value between 15 and 19%. The weight loss values are slightly higher than the PLA content in the PU foams probably because some tiny particles were washed away. Therefore, the polyurethane foams containing PPO-*b*-PLA block copolymers exhibit significantly improved degradability when compared with commonly used polyurethane foams.

CONCLUSIONS

Degradable PPO-*b*-PLA copolymers are prepared by ring-opening polymerization of lactide using stannous octoate as catalyst and low unsaturated PPO triol as macroinitiator. DSC results show that the T_g of the copolymers increases with increasing the PLA content. The PPO-*b*-PDLLA copolymers are intrinsically amorphous. In contrast, the PPO-*b*-PLLA copolymers are semicrystalline, and higher T_m and crystallinity are obtained with increasing the PLLA segment length. WAXD spectra of the PPO-*b*-PLLA copolymers exhibit two main peaks at 16.8° and 19.2°, belonging to the (110)/(200) and (203) reflections of α crystal cell of PLLA. Thermal

decomposition data confirm that the thermal stability of the block copolymers can be improved by introducing PLA segments. Polyurethane foams containing the PPO-*b*-PLA copolymers are synthesized. Alkaline hydrolysis experiments proved that the polyurethane foams containing PPO-*b*-PLA copolymers exhibit a partial degradability. Therefore, these novel copolymers present a potential as environmentally friendly materials.

References

1. Nagahama, K.; Nishimura, Y.; Ohya, Y.; Ouchi, T. Polymer 2007, 48, 2649.
2. Lemmouchi, Y.; Perry, M. C.; Amass, A. J.; Chakraborty, K.; Schacht, E. J Polym Sci Part A: Polym Chem 2007, 45, 3966.
3. Stefani, M.; Coudane, J.; Vert, M. Polym Degrad Stab 2006, 91, 2554.
4. Sunder, A.; Mülhaupt, R.; Frey, H. Macromolecules 2000, 33, 309.
5. Kulinski, Z.; Piorkowska, E.; Gadzinowska, K.; Stasiak, M. Biomacromolecules 2006, 7, 2128.
6. Piorkowska, E.; Kulinski, Z.; Galeski, A.; Masirek, R. Polymer 2006, 47, 7178.
7. Chisholm, M. H.; Navarro-Llobet, D.; Simonsick, W. J. Macromolecules 2001, 34, 8851.
8. Aubrecht, K. B.; Grubbs, R. B. J Polym Sci Part A: Polym Chem 2005, 43, 5156.
9. Saiani, A.; Novak, A.; Rodier, L.; Eeckhaut, G.; Leenslag, J. W.; Higgins, J. S. Macromolecules 2007, 40, 7252.
10. Williams, S. R.; Mather, B. D.; Miller, K. M.; Long, T. E. J Polym Sci Part A: Polym Chem 2007, 45, 4118.
11. Nomura, Y.; Sato, A.; Sato, S.; Mori, H.; Endo, T. J Polym Sci Part A: Polym Chem 2007, 45, 2689.
12. van der Schuur, M. J.; Gaymans, R. J. Polymer 2007, 48, 1998.
13. Cuscurida, M. U.S. Pat. 3,393,243 (1968).
14. Heuvelsland, A. J. E.P. Pat. 0,369,487 (1990).
15. Olstowski, F.; Nafziger, J. L. U.S. Pat. 4,282,387 (1981).
16. Pazos, J. F.; Shih, T. T. U.S. Pat. 5,689,012 (1997).
17. Le-Khac, B. U.S. Pat. 5,470,813 (1995).
18. Le-Khac, B. U.S. Pat. 5,482,908 (1996).
19. Tuinman, R.; Fishback, T. L.; Reichel, C. J. U.S. Pat. 6,344,494 (2002).
20. Tuinman, R.; Lee, T. B.; Fishback, T. L.; Reichel, C. J. U.S. Pat. 6,201,035 (2001).
21. Yang, D. M.; Fan, Z. Y.; Tu, J. J.; Shi, Z. J.; Wang, W.; Yu, Y. J Fudan Univ 2006, 45, 380.
22. Rashkov, I.; Manolova, N.; Li, S. M.; Espartero, J. L.; Vert, M. Macromolecules 1996, 29, 50.
23. Kim, S. H.; Han, Y. K.; Ahn, K. D.; Kim, Y. H.; Chang, T. Makromol Chem 1993, 194, 3229.
24. Arvanitoyannis, I.; Nakayama, A.; Kawasaki, N.; Yamamoto, N. Polymer 1995, 36, 2947.
25. Yang, L.; Heatley, F.; Blease, T. G.; Thompson, R. I. G. A. Eur Polym J 1996, 32, 535.
26. Loh, X. J.; Tan, Y. X.; Li, Z.; Teo, L. S.; Goh, S. H.; Li, J. Biomaterials 2008, 29, 2164.
27. Flory, P. J. Principles of Polymer Chemistry; Cornell University Press: New York, 1953.
28. Hoffman, J. D.; Miller, R. L. Polymer 1997, 38, 3151.
29. Vasanthakumari, R.; Pennings, A. J. Polymer 1983, 24, 175.
30. Pyda, M.; Bopp, R. C.; Wunderlich, B. J Chem Therm 2004, 36, 731.
31. Day, M.; Nawaby, A. V.; Liao, X. J Therm Anal Cal 2006, 86, 623.
32. De Santis, P.; Kovacs, A. J. Biopolymers 1968, 6, 299.
33. Kobayshi, J.; Asahi, T.; Ichiki, M.; Oikawa, A.; Suzuki, H.; Watanabe, T.; Fukada, E.; Shikinami, Y. J Appl Phys 1995, 77, 2957.
34. Hoogsteen, W.; Postema, A. R.; Pennings, A. J.; Ten Brinke, G.; Zugenmaier, P. Macromolecules 1990, 23, 634.
35. Eling, B.; Gogolewski, S.; Pennings, A. J. Polymer 1982, 23, 1587.
36. Puiggali, J.; Ikada, Y.; Tsuji, H.; Cartier, L.; Okihara, T.; Lotz, B. Polymer 2000, 41, 8921.
37. Sawai, D.; Takahashi, K.; Imamura, T.; Nakamura, K.; Kanamoto, T.; Hyon, S. H. J Polym Sci Part B: Polym Phys 2002, 40, 95.
38. Sawai, D.; Takahashi, K.; Sasashige, A.; Kanamoto, T.; Hyon, S. H. Macromolecules 2003, 36, 3601.
39. Garkhal, K.; Verma, S.; Jonnalagadda, S.; Kumar, N. J Polym Sci Part A: Polym Chem 2007, 45, 2755.
40. Pan, P.; Kai, W.; Zhu, B.; Dong, T.; Inoue, Y. Macromolecules 2007, 40, 6898.
41. Wu, T.; He, Y.; Fan, Z. Y.; Wei, J.; Li, S. M. Polym Eng Sci 2008, 48, 425.